

COMPUTATIONAL METHODS AND RESULTS FOR STRUCTURED MULTISCALE MODELS OF TUMOR INVASION*

BRUCE P. AYATI[†], GLENN F. WEBB[‡], AND ALEXANDER R. A. ANDERSON[§]

Abstract. We present multiscale models of cancer tumor invasion with components at the molecular, cellular, and tissue levels. We provide biological justifications for the model components, present computational results from the models, and discuss the scientific-computing methodology used to solve the model equations. The models and methodology presented in this paper form the basis for developing and treating increasingly complex, mechanistic models of tumor invasion that will be more predictive and less phenomenological. Because many of the features of the cancer models, such as taxis, aging, and growth, are seen in other biological systems, the models and methods discussed here also provide a template for handling a broader range of biological problems.

Key words. tumor invasion, physiological structure

AMS subject classifications. 92-08, 92C50, 92C37, 35Q80, 35M10, 65-04

DOI. 10.1137/050629215

1. Introduction. In this paper we present multiscale models of cancer tumor invasion and the scientific-computing methodology for solving the model equations. The specific model treated here has components at the molecular level (incorporated via diffusion and taxis processes), the cellular level (incorporated via a cell age variable), and the tissue level (incorporated via spatial variables). The tumor consists of populations of proliferating and quiescent cells. Proliferating cells are capable of growing, dividing, entering quiescence, and becoming necrotic. We consider one mutation class of proliferating and quiescent cells. The different physical scales cause the model to have widely different time scales. The fully continuous model treated in detail in this paper depends on variables representing time, age, and two spatial dimensions. We present this system as a simplification of a more general system that depends on time, age, size, and three spatial dimensions, and has an arbitrary number of mutation classes for proliferating and quiescent cells, with increasingly aggressive invasion characteristics. Mathematical modeling of all phases of cancer tumor development, angiogenesis, and metastasis is a very broad and active area of mathematical biology [1, 5, 10, 16, 35, 51].

This paper focuses on the invasion of nearby tissue by a vascular tumor, under the assumption that the surrounding tissue is the source of the vasculature. Our fully continuous models have components that are based on hybrid discrete-continuous (HDC) models [2, 3, 4, 6, 7] which use a discrete lattice to represent space. We use a physiological variable, age, to model aging in the proliferating and quiescent tumor cell populations [26, 34]. The models in this paper belong to the class of so-called structured population models in which individuals in a population are tracked by properties such as age, size, maturity, and other quantifiable variables. Diffusion and haptotaxis terms

*Received by the editors April 14, 2005; accepted for publication (in revised form) August 24, 2005; published electronically January 27, 2006.

<http://www.siam.org/journals/mms/5-1/62921.html>

[†]Department of Mathematics, Southern Methodist University, Dallas, TX 75205 (ayati@smu.edu).

[‡]Department of Mathematics, Vanderbilt University, Nashville, TN 37240 (glenn.f.webb@vanderbilt.edu). This author was supported by PHS-NIH grant 1P50CA113007-01.

[§]Division of Mathematics, University of Dundee, Dundee DD1 4HN, Scotland (anderson@maths.dundee.ac.uk). This author was supported by PHS-NIH grant 1P50CA113007-01.

account for the spatial dynamics of the system in the models under study. Age, size, and/or space structure have also been used in models of tumor cords [17, 18, 19, 27].

Computational and software considerations often limit scientists from incorporating physiological structure directly into a model. We discuss the combination of effective computational methodologies for integration over the time, age, and space variables; we use a moving-grid Galerkin method for the age variable, an adaptive step-doubling method for the time variable, and an alternating direction implicit (ADI) scheme for the space variables.

This paper is organized into three main sections. The first develops the models and presents their biological justifications. The second section presents computed solutions to the model equations and discusses their significance. The third section discusses the computational methodology. We close with a section on conclusions and further research.

2. Model equations. We extend the HDC tumor invasion model discussed in [4] to fully deterministic models. In particular, as with [4], we focus on four key variables implicated in the invasion process: tumor cells, surrounding tissue (extracellular matrix), matrix degradative enzymes, and oxygen. Tumor cell motion in the HDC model is driven by a mixture of both biased and unbiased migration, where the biased migration is assumed to be from haptotaxis (in response to gradients in the surrounding tissue) and the unbiased migration is just random motility; we shall assume the same here. We assume as in [4] that tumor cells produce matrix degrading enzymes which in turn degrade the surrounding tissue creating gradients for the cells to respond to haptotactically. Oxygen production is assumed to be proportional to the tissue density and to be consumed by the tumor (see [4] and the references therein for a more detailed explanation of the HDC model derivation).

One of the important features of the model proposed in [4] was the implementation of tumor heterogeneity; i.e., the tumor is made up of many different subpopulations with different phenotypes. These phenotypes allow us to model subpopulations with different invasive capacities. We use the same idea here by considering multiple populations of tumor cells with potentially different parameter values.

Since the models we present here are continuous in all variables, individual processes of the tumor cells (such as division) are also considered to be continuous. These are modeled according to cell age in the simplified model used in the computations, and cell age and size in the more general system. As with the HDC model, these models are based on the populations of proliferating and quiescent tumor cells, the density of surrounding tissue macromolecules, the concentration of matrix degradative enzyme, and the concentration of oxygen.

The general class of partial differential equations for diffusion and age structure considered in this paper has a long history. Among the first classic works are Skellam (1951) [56] (who considered the effects of diffusion on populations), Sharpe and Lotka (1911) [55], and McKendrick (1926) (who considered population models with linear age structure) [49, 63]. More recently, Gurtin and MacCamy [32] considered models with nonlinear age structure. Rotenberg [53] and Gurtin [31] posed models dependent on both age and space. Gurtin and MacCamy [33] differentiated between two kinds of diffusion in these models: diffusion due to random dispersal and diffusion toward an area of less crowding. Existence and uniqueness results can be found for various forms of these models in Busenberg and Iannelli [21], di Blasio [23], di Blasio and Lamberti [24], Langlais [43], MacCamy [47], and Webb [62]. Further analysis has been done by several authors [36, 41, 44, 48].

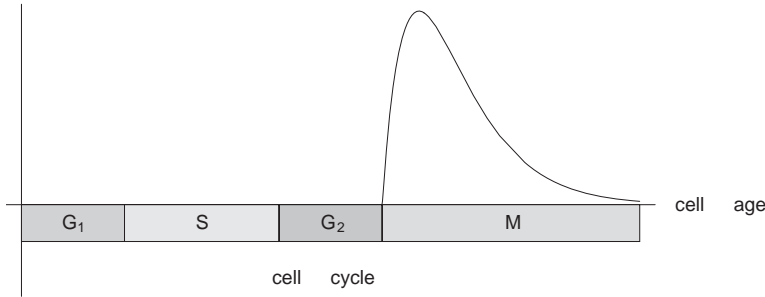


FIG. 1. Schematic of the phases G_1 (first gap), S (synthesis), G_2 (second gap), and M (mitosis) of the cell cycle correlated to cell age. The graph over the mitotic phase corresponds to the probability density function of cell ages at division (the response of the function θ to age).

2.1. The age-, space-, and size-structured model of tumor invasion. The tumor is contained in a region of tissue Ω . The tumor is composed of proliferating cells (cells that are transiting the cell cycle to mitosis) and quiescent cells (cells that are arrested in the cycle but are capable of resuming progress). We assume that proliferating cells are motile in space, but quiescent cells are not, and that both proliferating and quiescent cells consume oxygen, with quiescent cells at a lower rate (as in [4]). Cells, both proliferating and quiescent, are distinguished by their position $x \in \Omega$, their age a between 0 (newly divided) and a_M (maximum possible age), their size s between s_m (minimum possible size) and s_M (maximum possible size), and their state in the mutation sequence. Cell age, for both proliferating cells and quiescent cells, is the time since the cell was newly divided. For proliferating cells, cell age correlates to phase of the cell cycle (first gap G_1 , synthesis S , second gap G_2 , and mitosis). An illustration of a distribution of division ages is given in Figure 1. Cells are also distinguished by cell size, which can be interpreted as mass, diameter, volume, or some other measurable property. The inclusion of cell age and cell size allows description of the growth of the tumor mass to be understood at the level of individual cells, as they double their size and divide into two new daughter cells. For example, the inclusion of age and size in the diffusivities represents a means by which growing and dividing cells increase total tumor size.

In the HDC model in [4], the behavior of individual cells is tracked cell by cell on a spatial lattice. This discrete formulation relates detailed information about fundamental processes at the cellular level, such as cell-cell adhesion, entry to and from quiescence, division, apoptosis, and phenotype mutation, to behavior of the tumor mass. In the continuous age-size structured model of this paper, behavior at the population level is also related to behavior at the individual cell level, with cell age and size-dependent densities providing the connection to these processes. The use of continuous densities constitutes a local averaging of individual traits.

The dependent variables of the model are the following:

- $p_i(x, a, s, t)$ = density of proliferating tumor cells of type i in the tumor at position x , age a , and size s at time t , where $i = 0$ corresponds to a mutated type p53 gene, and $i = 1, 2, \dots, n$ corresponds to a linear sequence of mutated phenotypes of increasing aggressiveness. The number of mutations can be very large, with successive phenotypes possessing greater proliferative characteristics and capacity for spatial movement.

- $q_i(x, a, s, t)$ = density of quiescent tumor cells of type i in the tumor at position x , age a , size s , and mutation phenotype $i = 0, 1, 2, \dots, n$ at time t .
- $f(x, t)$ = surrounding tissue macromolecule (MM) density at position x at time t . It is assumed that these MM are distributed heterogeneously in Ω but immobile in Ω .
- $m(x, t)$ = matrix degradative enzyme (MDE) concentration at position x at time t . MDE is produced by the tumor cells and diffuses in Ω .
- $c(x, t)$ = oxygen concentration at position x at time t . Oxygen is produced by the extracellular MM, diffuses in Ω , and is consumed by the tumor cells.
- $P(x, t) = \sum_{i=0}^n \int_0^{a_M} \int_{s_m}^{s_M} p_i(x, a, s, t) ds da$ = the total population density in x of proliferating cells of all types at time t .
- $Q(x, t) = \sum_{i=0}^n \int_0^{a_M} \int_{s_m}^{s_M} q_i(x, a, s, t) ds da$ = the total population density in x of quiescent cells of all types at time t .
- $N(x, t) = P(x, t) + Q(x, t)$ = total tumor population density in x of all cell types at time t .

We use a single maximum age and size for all cell types and mutation classes. This is a notational convenience; models are often written with unbounded age or size domains under the quite reasonable assumption that biological entities do not grow or age indefinitely due to death. Thus, the domain can be truncated at the numerical level. A mathematical treatment on truncating an infinite age domain is provided in [12]. In this paper we choose to define these parameters beforehand and use the largest values we need to cover all cases.

The equations governing the proliferating-cell densities of the tumor are

(2.1a)

$$\begin{aligned}
\frac{\partial}{\partial t} p_i(x, a, s, t) = & - \underbrace{\frac{\partial}{\partial a} p_i(x, a, s, t)}_{\text{cell aging}} - \underbrace{\frac{\partial}{\partial s} (\kappa_i(a, s, c) p_i(x, a, s, t))}_{\text{cell growth}} \\
& + \underbrace{\nabla \cdot (D_{p_i}(x, a, s, N) \nabla p_i(x, a, s, t))}_{\text{diffusion}} - \underbrace{\chi_i \nabla \cdot (p_i(x, a, s, t) \nabla f(x, t))}_{\text{haptotaxis}} \\
& - \underbrace{\rho_i(x, a, s, c, N) p_i(x, a, s, t)}_{\text{cell death from insufficient oxygen}} - \underbrace{\theta_i(x, a, s, c, N) p_i(x, a, s, t)}_{\text{division with sufficient oxygen}} \\
& - \underbrace{\sigma_i(x, a, s, c, N) p_i(x, a, s, t)}_{\text{exit to quiescence}} + \underbrace{\tau_i(x, a, s, c, N) q_i(x, a, s, t)}_{\text{entry from quiescence}},
\end{aligned}$$

with age-boundary conditions

$$\begin{aligned}
(2.1b) \quad \underbrace{p_i(x, 0, s, t)}_{\text{newborn type } i \text{ cells}} = & 4(1 - \psi_i) \underbrace{\int_0^{a_M} \theta_i(x, a, 2s, c, N(x, t)) p_i(x, a, 2s, t) da}_{\text{type } i \text{ cell division}} \\
& + 4\psi_{i-1} \underbrace{\int_0^{a_M} \theta_{i-1}(x, a, 2s, c, N(x, t)) p_{i-1}(x, a, 2s, t) da}_{\text{type } i-1 \text{ cell division}},
\end{aligned}$$

where ψ_i is the fraction of type i cells with type $i + 1$ mutation. The variable a in (2.1b) is the variable of integration over all ages. For cells that have undergone only one primary cancer forming mutation (such as a p53 mutation), we set $i = 0$ and $\psi_{-1} = 0$. The coefficient of 4, rather than the more intuitive doubling value of 2,

results from the assumption of size symmetric cell division; asymmetric cell division would require a mitosis kernel and integration over a size variable u in (2.1b) [64]. That is, if $k(s, u)$ is the probability density function for a daughter cell of size s to result from the division of a mother cell of size u , then $k(s, u) = k(u-s, u)$. Symmetric division means that $k(s, u) = \delta(s - \frac{u}{2})$, where δ is the Dirac delta function. Thus, for symmetric division, the rate at which daughter cells of size s are born from mother cells of size $2s$ satisfies

$$\begin{aligned} & 2 \int_{s_m}^{s_M} \int_0^{a_M} k(s, u) \theta_i(x, a, u, c, N(x, t)) p_i(x, a, u, t) da du \\ &= 2 \left(2 \int_{s_m}^{s_M} \int_0^{a_M} \delta(s - \hat{u}) \theta_i(x, a, 2\hat{u}, c, N(x, t)) p_i(x, a, 2\hat{u}, t) da d\hat{u} \right) \\ &= 4 \int_0^{a_M} \theta_i(x, a, 2s, c, N(x, t)) p_i(x, a, 2s, t) da. \end{aligned}$$

The equations governing the quiescent-cell densities are

$$(2.1c) \quad \frac{\partial}{\partial t} q_i(x, a, s, t) = - \underbrace{\frac{\partial}{\partial a} q_i(x, a, s, t)}_{\text{cell aging}} - \underbrace{\nu_i(x, a, s, c, N(x, t)) q_i(x, a, s, t)}_{\text{cell death from insufficient oxygen}} \\ + \underbrace{\sigma_i(x, a, s, c, N(x, t)) p_i(x, a, s, t)}_{\text{entry from proliferation}} - \underbrace{\tau_i(x, a, s, c, N(x, t)) q_i(x, a, s, t)}_{\text{exit to proliferation}}.$$

The quiescent-cell populations lack a boundary condition in age since they are “born” when proliferating cells of the same mutation class become quiescent. As mentioned above, age in (2.1a)–(2.1c) is time since mitosis and does not change the instant cells transit between proliferating or quiescent states.

The equations governing tissue MM, MDE, and oxygen densities are precisely those used in [4]:

$$(2.1d) \quad \frac{\partial}{\partial t} f(x, t) = - \underbrace{\delta m(x, t) f(x, t)}_{\text{degradation}},$$

$$(2.1e) \quad \frac{\partial}{\partial t} m(x, t) = \underbrace{D_m \nabla^2 m(x, t)}_{\text{diffusion}} + \underbrace{\mu P(x, t) + \omega Q(x, t)}_{\text{production}} - \underbrace{\lambda m(x, t)}_{\text{decay}},$$

$$(2.1f) \quad \frac{\partial}{\partial t} c(x, t) = \underbrace{D_c \nabla^2 c(x, t)}_{\text{diffusion}} + \underbrace{\beta f(x, t)}_{\text{production}} - \underbrace{\gamma P(x, t) - \eta Q(x, t)}_{\text{uptake}} - \underbrace{\alpha c(x, t)}_{\text{decay}}.$$

Equations (2.1a)–(2.1f) are combined with initial conditions and no-flux boundary conditions on the boundary $\partial\Omega$ of Ω .

Equation (2.1a) balances the way cells age, grow, and move in time. The first term on the right-hand side of (2.1a) accounts for the aging of cells, which is one-to-one with advancing time. In the second term in (2.1a), $\kappa_i(a, s, c)$ is the rate at which proliferating cells increase size; i.e., $\int_{s_1}^{s_2} \frac{1}{\kappa_i(a, s, c)} ds$ is the time required for a cell of type i to grow from size s_1 to size s_2 .

The diffusion term in (2.1a) accounts for cell movement due to random motility,

interphase drag, the interaction between cells, volume displacement due to cell division, and cell-cell adhesion [10]. The diffusion coefficient $D_{p_i}(x, a, s, N(x, t))$ can be allowed to depend on the independent and dependent variables to incorporate mechanistic features of these processes. For example, cells in higher mutation phenotype classes may have smaller cell-cell adhesion properties, and thus have a larger coefficient. Dividing cells of larger size may exert greater force of volume displacement, and thus have a larger coefficient.

In (2.1a), the haptotaxis term represents directed movement of cells toward concentrations of MM, which is the source of oxygen necessary for tumor cell growth, and is degraded by tumor cell produced MDE. The parameter χ_i is the haptotaxis coefficient.

The coefficient $\rho_i(x, a, s, c, N(x, t))$ of proliferating cell loss in (2.1a) is dependent on the density of cells in competition for the supply of oxygen.

In (2.1b), $\theta_i(x, a, s, c, N(x, t))$ is the rate at which cells of type i , age a , and size s divide at x per unit time, where it is assumed that a mother cell divides into two daughter cells of equal size (unequal division can also be modeled [64]). The division rate $\theta_i(x, a, s, c, N(x, t))$ depends on the age of cells, the supply of oxygen, and the density of cells, with reduced capacity for division as the oxygen supply decreases and the density increases. The negative sign in front of $\theta_i(x, a, s, c, N(x, t))$ reflects the loss of cells due to the division process. The mother cell of age a and size s is replaced by two daughter cells, each having age 0 and half the size of the mother cell, as described in the boundary condition (2.1b).

The coefficients $\sigma_i(x, a, s, c, N(x, t))$ and $\tau_i(x, a, s, c, N(x, t))$ of transition to and from quiescence in (2.1a) depend on the supply of oxygen and the density of tumor cells. Lower oxygen and higher density results in increased entry to quiescence, and higher oxygen and lower density results in increased recruitment from quiescence.

Equation (2.1c) governing the quiescent cells is interpreted similarly, where it is assumed that quiescent cells are not motile. In this model, we represent the properties of individual cell behavior as rates of transition dependent on cell spatial position, age, and size. The inclusion of cell age and size structure allows incorporation of cell level processes without tracking of each cell history, cell by cell (as is done in [4]). The hybrid and continuum modeling approaches have complementarity in development, analysis, and computability, in which advantages of each can be exploited.

2.2. A simplified two-dimensional model with no size structure. The following model is a version of the model above with no size structure, two spatial dimensions (denoted by $(x, y) \in \Omega$), and one compartment each of proliferating- and quiescent-cell types. The equations governing the two classes of cell densities of the tumor are

$$\begin{aligned}
 \frac{\partial}{\partial t} p(x, y, a, t) = & - \underbrace{\frac{\partial}{\partial a} p(x, y, a, t)}_{\text{cell aging}} \\
 (2.2a) \quad & + \underbrace{D_p \nabla^2 p(x, y, a, t)}_{\text{diffusion}} - \underbrace{\chi \nabla \cdot (p(x, y, a, t) \nabla f(x, y, t))}_{\text{haptotaxis}} \\
 & - \underbrace{\rho(x, y, a, c) p(x, y, a, t)}_{\text{cell death from insufficient oxygen}} - \underbrace{\theta(x, y, a, c) p(x, y, a, t)}_{\text{division with sufficient oxygen}} \\
 & - \underbrace{\sigma(x, y, a, c, N(x, t)) p(x, a, s, t)}_{\text{exit to quiescence}} + \underbrace{\tau(x, y, a, c) q(x, y, a, t)}_{\text{entry from quiescence}},
 \end{aligned}$$

$$(2.2b) \quad \frac{\partial}{\partial t} q(x, y, a, t) = - \underbrace{\frac{\partial}{\partial a} q(x, y, a, t)}_{\text{cell aging}} - \underbrace{\nu(x, y, a, c) q(x, y, a, t)}_{\text{cell death from insufficient oxygen}} \\ + \underbrace{\sigma(x, y, a, c, N(x, t)) p(x, y, a, t)}_{\text{entry from proliferation}} - \underbrace{\tau(x, y, a, c) q(x, y, a, t)}_{\text{exit to proliferation}},$$

with age-boundary conditions

$$(2.2c) \quad \underbrace{p(x, y, 0, t)}_{\text{newborn cells}} = 2 \underbrace{\int_0^{a_M} \theta(x, y, a, c) p(x, y, a, t) da}_{\text{division rate}}.$$

The equations governing tissue MM (f), MDE (m), and oxygen (c) densities remain as defined in (2.1d)–(2.1f). All equations are combined with initial conditions and zero flux boundary conditions on an (x, y) -rectangle Ω .

In this simplification, the use of age as a proxy for size has been chosen to illustrate the capabilities of the modeling framework and computational methodology and to form a foundation for further research. Our simplification is mathematical: we remove only the size dimension and size derivative in (2.1a) to obtain a system soluble by our current methodology and software. The modeling implication of this simplification is that proliferating and quiescent cells differ from one another only in the ability of the former to diffuse and haptotaxi. In (2.1a)–(2.1c), proliferating and quiescent cells also differ in the ability of the former to grow in size.

There are many paths from very simple tumor models—models where the cell population is completely homogeneous and evolves according to an ordinary differential equation—and the model presented in (2.1a)–(2.1f) where we differentiate between cells based on age, size, spatial position, proliferating or quiescent state (including which differences between them to retain), and mutation class. Another path would be to dispense with age representing time since mitosis in (2.1a)–(2.1c) and replace the size variable by an age variable which represents time spent in the proliferation class. This would reduce (2.1c) to an ordinary differential equation with q parameterized by space (x, y) and age a . An intermediary model between (2.1a)–(2.1c) and (2.2a)–(2.2b) would be to keep the age variable as it is and replace the size variable by a second age variable representing time spent in the proliferation class.

3. Computations of cancer tumor invasion. We can demonstrate some aspects of the behavior of the reduced system defined by (2.2a)–(2.2c) and (2.1d)–(2.1f) through computations using parameters and functional forms chosen for illustrative purpose rather than biological foundation, including choices such as the relative death rates of proliferating and quiescent cells. Models in later work will be nondimensional versions of dimensional models whose parametric input will be experimentally validated in the future. The magnitude of some dimensional parameters is provided on p. 168 of [4].

We take the spatial domain to be $\Omega = [-5, 5] \times [-5, 5]$, bound the age domain by $a_M = 6$, and run the computations to time $t = 20$. We now replace the vector x denoting space with an ordered pair of real numbers (x, y) . The meaning of x should be clear from context.

We take

$$(3.1a) \quad D_p = 0.0005, \quad \chi = 0.01, \quad D_m = 0.01, \quad D_c = 0.05,$$

$$(3.1b) \quad \rho(x, y, c) = 0.1 \max\{1.0 - c, 0\}, \quad \nu(x, y, c) = 2.0 \max\{1.0 - c, 0\},$$

$$(3.1c) \quad \delta(x, y) = 50.0, \quad \mu(x, y) = 1.0, \quad \omega(x, y) = 0.0, \quad \lambda(x, y) = 0.0,$$

$$(3.1d) \quad \beta(x, y) = 0.5, \quad \gamma(x, y) = 0.57, \quad \eta(x, y) = 0.0, \quad \alpha(x, y) = 0.025,$$

$$(3.1e) \quad \sigma(x, y, c) = 10.0 \max\{1.0 - c, 0\}, \quad \tau(x, y, c) = 2.0 c.$$

The distribution of division ages is assumed to have the form of an offset integrand of the Gamma function (see Figure 1),

$$(3.1f) \quad \theta(x, y, a, c) = \begin{cases} 10.0 c \exp(-10(a-1)) (2a-1)^5, & a > 0.5, \\ 0, & a < 0.5, \end{cases}$$

where 0.5 is the minimum age at which a cell can divide. The initial conditions are

$$(3.1g) \quad p(x, y, a, 0) = 5.0 G(\sqrt{x^2 + y^2}, 0, 0.5),$$

$$(3.1h) \quad q(x, y, a, 0) = 0.5 p(x, y, 0)$$

for $0 \leq a \leq 2$, $p(x, y, a, 0) = q(x, y, a, 0) = 0$ otherwise,

$$(3.1i) \quad f(x, y, 0) = 0.2 \cos(0.4(x-5)^2) \sin(0.2(y-5)^2) + 0.2,$$

$$(3.1j) \quad m(x, y, 0) = 2.5 G(\sqrt{x^2 + y^2}, 0, 0.5),$$

$$(3.1k) \quad c(x, y, 0) = 10.0 f(x, y, 0),$$

where

$$G(z, z_\mu, z_\sigma) = \frac{\exp(-\frac{(z-z_\mu)^2}{2z_\sigma^2})}{\sqrt{2\pi} z_\sigma}.$$

Numerical computations of the proliferating-cell density and MM density for the simplified model are illustrated in Figures 3–5 as snapshots in time.¹ The simulation in Figures 2–5 demonstrates the temporal development of spatial heterogeneity in the tumor mass from a radially symmetric initial condition of tumor cells and heterogeneous initial condition of surrounding MM. The MM tissue is displaced by the tumor tissue as a consequence of haptotactic movement of the tumor cells, driven by the MDE they produce. The interior core of the tumor mass becomes necrotic, because of its increasing distance from the oxygen supply provided by the MM source. One aspect of this computation is that the tumor edge consists of an outer layer of proliferating cells and an inner layer of quiescent cells. This phenomenon was obtained despite differentiating proliferating cells from quiescent cells only by their ability to diffuse and haptotaxi.

4. Computational methodology. Computational robustness and efficiency is vital for the methods used to solve the high-dimension, multiscale models developed in this paper. The primary issue is the age discretization and how to decouple it from the time discretization without ignoring the fact that age and time advance together. This approach foreshadows how one may wish to handle size structure. The decoupling of the age and time discretizations allows for adaptivity in the time variable; we discuss a particularly effective method for the time integration called step-doubling. The third computational consideration is in how we solve the system

¹Animations can be found online at <http://faculty.smu.edu/ayati/cancer.html>.

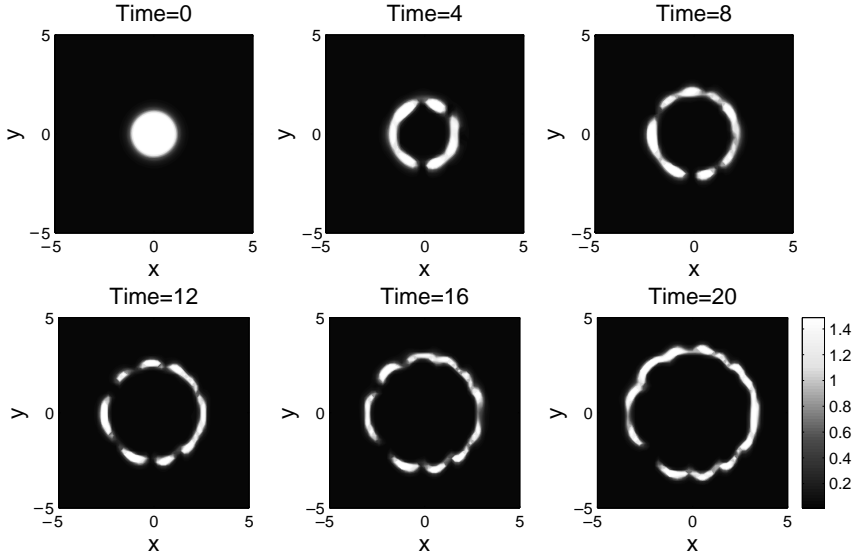


FIG. 2. Tumor-cell density (N) for the system defined by (2.2a)–(2.2c) and (2.1d)–(2.1f). The parameters used in this computation are defined in (3.1a)–(3.1k).

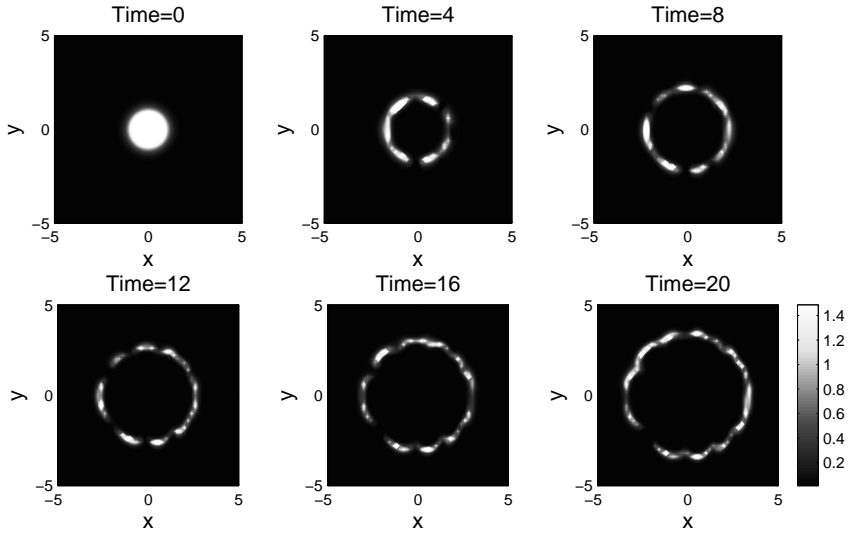


FIG. 3. Proliferating-cell density (P) for the system defined by (2.2a)–(2.2c) and (2.1d)–(2.1f). The parameters used in this computation are defined in (3.1a)–(3.1k).

in the space variables. We use an alternating direction implicit method, which is, to our knowledge, a novel approach when incorporated into the step-doubling method for time.

There is a plethora of numerical methods for solving models with just age or size structure [8, 9, 22, 29, 37, 42, 46, 58]. These methods use uniform age and time steps which are equal to one another in the case of age structure, or they do the equivalent

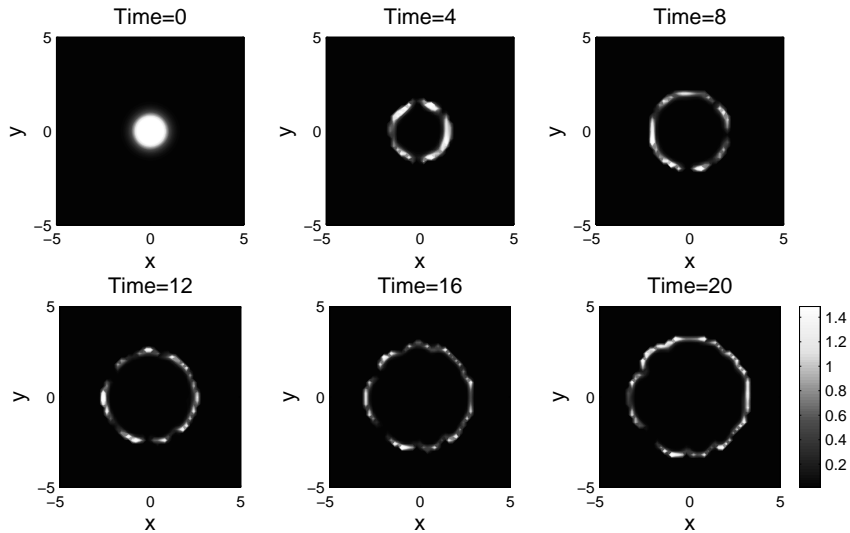


FIG. 4. Quiescent-cell density (Q) for the system defined by (2.2a)–(2.2c) and (2.1d)–(2.1f). The parameters used in this computation are defined in (3.1a)–(3.1k).

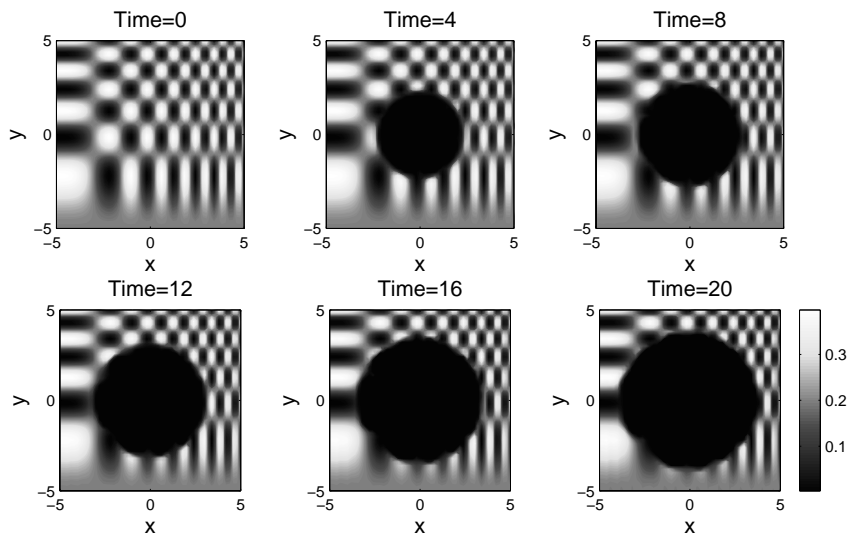


FIG. 5. MM density (f) for the system defined by (2.2a)–(2.2c) and (2.1d)–(2.1f). The parameters used in this computation are defined in (3.1a)–(3.1k).

in the context of size structure of introducing a new size node at every time step. This approach does not work well for problems with multiple time scales because the fastest time scale tends to be in the spatial variables.

To understand the nature of this problem, consider a fixed, uniform age discretization. Solving the system along characteristics would require the age interval width to be equal to the time step. This would result in many more age nodes than are needed to accurately solve the problem in the age variable because of the small time

step. For size structure, the analogous situation is to introduce many more size nodes at the birth boundary than are needed. An additional concern with size structure is that characteristic curves in the size-time plane can converge, resulting in unnecessarily narrow size intervals. Regridding was used in [58] and [9] to adjust for the effects of narrowing gaps between characteristics, but they do not address the issue of small size nodes at the birth boundary. For example, the method proposed in [9] has an advantage of simplicity—the idea is to merge the narrowest size interval with one of its neighbors after each time step—but is not a satisfactory solution because small size intervals can arise continuously at the birth boundary while elsewhere size intervals continue to narrow due to the nature of the characteristic curves. Moreover, regridding comes at a computational cost. A natural solution to this problem lies in using a finite element space with a moving reference frame in age or size, which is the approach we use in this paper.

Previous numerical methods designed explicitly for models with dependence on age, time, and space were developed outside the context of an application and required uniform age and time discretizations with the age step chosen to equal the time step [39, 40, 45]. In contrast, the methods used to obtain the computational results presented in this paper [12, 14] were motivated by models of *Proteus mirabilis* swarm-colony development where the need to decouple age and time discretizations was clear from the problem [13, 28, 52]. In the process of applying these methods to the system defined in [28], it became clear that the numerical methods and software used previously were not merely inefficient but also gave qualitatively incorrect answers (although these methods did decouple the age and time discretizations, they did so by not moving the age discretization along characteristics; see the appendix in [13] for a discussion). This is a critical pitfall to avoid and highlights the importance of using methods with known convergence properties for a particular system.

We use Galerkin finite element methods that use a moving grid to allow for independent, nonuniform age and time discretizations and whose development has focused on robustness as well as computational efficiency. The important property of these methods is that the age step need not equal the time step. Instead, the positions of the age nodes are adjusted by the time step. The methods preserve the important fact that age and time advance together. The methods in [39, 40, 45] also discretized along characteristics, but they did so simultaneously in age and time and thus imposed the often crippling constraint that the time and age steps be both constant and equal. The difficulty with this approach is twofold. First, the use of constant age and time steps prevents adaptivity of the discretization in age or, especially, time. Second, and more importantly, the coupling of the age and time meshes can cause great losses of efficiency since only rarely will the dynamics in time be on the same scale as the dynamics in age. This is particularly the case when space is involved since sharp moving fronts can require small time steps, whereas the behavior in the age variable can remain relatively smooth. The age discretization presented in [39, 40, 45] can be viewed as special cases of the methods presented in [12, 14] by setting the time and age meshes to be constant and equal and using a backward Euler discretization in time and a piecewise constant finite element space in age.

Step-doubling [15, 30, 54] is a conceptually simple, yet quite effective method for the adaptive time integration of differential equations. Over a time step, we compute one solution over the entire time step and then a second solution over two successive half steps. These two different solutions give us two things. First, we can compare solutions to determine the accuracy of our approximation for the purposes of adaptivity of the time step. Second, we can combine solutions to get a likely second-

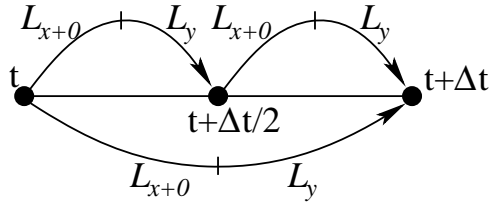


FIG. 6. Schematic of the combination of the step-doubling and ADI methods to advance the solution of a time- and space-dependent system from time t to time $t + \Delta t$. The operators L_{x+0} and L_y represent the x derivatives plus zero-order terms and the y derivatives, respectively.

order accurate approximation, even when each step in the step-doubling process is first-order accurate.

To solve the model equations in the spatial variables, we use an ADI method (also called operator splitting) where we first solve the equations in just the x derivatives and zero-order terms and then in just the y derivatives [25, 38, 50, 57, 59].

This approach reduces our two-dimensional problem in space to a set of more easily solved one-dimensional spatial problems; we need to solve a series of block tridiagonal linear systems instead of a more computationally expensive wide-banded linear system. Because ADI methods are time ordered, the ADI method needs to be embedded into the step-doubling algorithm.

The combination of these methods results in the following breakdown of the model equations. First, the moving-grid Galerkin methods in age reduce the age-, time-, and space-dependent equations to systems of differential equations that depend on time and two spatial variables. We then solve each of these equations by a combination of step-doubling and ADI methods; we take a step in the x -direction and zero-order terms, followed by a step in the y -direction, within each substep of step-doubling. This integrated stepping is illustrated in Figure 6.

The software used to generate the computed solutions in this paper has a similar structure to BuGS [11]. BuGS is a C++ toolkit for solving single space dimensional, nonlinear systems of partial differential equations which are at most order one in time and order two in space. The user defines the spatial discretization of the equations by writing a residual function based on first-order backward differences in time. BuGS then uses the step-doubling method described in [15] to get a second-order accurate in time implicit finite difference scheme. BuGS also features step control for the convergence of Newton's method and automatic approximation of the Jacobi matrix.

The age methods presented in [12, 14] use discontinuous piecewise polynomials as the basis functions for the age space, which results in a distinct system of parabolic partial differential equations for each age interval if we keep time and space continuous. This, in turn, results in a distinct linear system for each age interval when we fully discretize the equations. In the tumor invasion software, we use piecewise constant functions in age with postprocessing to continuous piecewise linear functions. As mentioned above, the tumor invasion software works by updating the age discretization at the beginning of a time step and then applying the step-doubling method to the subsystems corresponding to each age interval, splitting the spatial operator into two separate operators over each dimension.

As in BuGS, the tumor invasion software requires the user to define the spatial discretization of the equations by writing a residual function based on first-order backward differences in time. The software then uses the implementation of the step-

doubling method described in [15] to get a second-order accurate in time implicit finite difference scheme. The software also features step control for the convergence of Newton's method and automatic approximation of the Jacobi matrix.

In the remainder of this section we provide mathematical formulations of the moving-grid Galerkin methods used to reduce the age- and space-structured partial differential equations to systems of parabolic equations in time and space. We then discuss the step-doubling ADI combination used to solve the parabolic equations corresponding to each age cohort. We summarize the existing convergence results and present a heuristic “symbol” analysis for the synthesis of step-doubling and ADI. The notation in this section will not necessarily correspond to that in the rest of the paper.

The Galerkin formulation for the moving-grid age method is that given in [14]. We consider the age-dependent population model with nonlinear diffusion,

$$(4.1a) \quad \partial_t u + \partial_a u = \nabla \cdot (k(x, p) \nabla u) - \mu(x, a, p) u, \quad x \in \Omega, \quad a > 0, \quad t > 0,$$

where ∇ and $\nabla \cdot$ denote the gradient and the divergence, respectively, in x . The function $u(x, a, t)$ represents the distribution of individuals, $\Omega \subset \mathbb{R}^n$ represents the spatial domain, a represents age, and t represents time. The function $\mu > 0$ is the death rate. The total population density, p , is given by

$$(4.1b) \quad p(x, t) = \int_0^\infty u(x, a, t) da, \quad x \in \Omega, \quad t > 0.$$

We have a birth condition

$$(4.1c) \quad u(x, 0, t) = b(x, u(x, \cdot, t)), \quad x \in \Omega, \quad t > 0,$$

that is dependent on the entire population distribution. We note that b is an operator whose second argument is a function defined on \mathbb{R}^+ , where \mathbb{R}^+ denotes the nonnegative real numbers. The diffusion arises from the symmetric random motion of each individual (Fickian diffusion). We have a Neumann boundary condition, with ν denoting the outward normal to $\partial\Omega$,

$$(4.1d) \quad k(x, p) \nabla u \cdot \nu = 0, \quad x \in \partial\Omega, \quad a > 0, \quad t > 0,$$

that represents an isolated environment. The initial condition is

$$(4.1e) \quad u(x, a, 0) = u_0(x, a), \quad x \in \Omega, \quad a > 0.$$

We make several assumptions.

CONDITION 4.1. *There exist constants C_0 and C_1 such that for $(x, p) \in \Omega \times \mathbb{R}$, k satisfies $0 < C_0 \leq k(x, p) \leq C_1$ and μ satisfies $0 < C_0 \leq \mu(x, a, p) \leq C_1$ for all a .*

CONDITION 4.2. *The functions $k(x, p)$ and $\mu(x, a, p)$ are uniformly Lipschitz continuous with respect to p with Lipschitz constants K_k and K_μ , respectively. The derivative $\partial_p k(x, p)$ exists. The derivative $\partial_a \mu(x, a, p)$ exists and is uniformly bounded by C_1 as a function of all its arguments, and $\|\partial_a \mu(x, \cdot, p)\|_{L^2(\mathbb{R}^+)} \leq C_1$ uniformly as a function of x and p .*

CONDITION 4.3. *The birth condition, $b : \Omega \times (L^1(\mathbb{R}^+) \cap L^2(\mathbb{R}^+)) \rightarrow \mathbb{R}^+$, satisfies the Lipschitz condition*

$$\begin{aligned} & |b(x, \varphi(x, \cdot, t)) - b(x, \psi(x, \cdot, t))| \\ & \leq K_b \left((1 + \|\varphi\|_{L^1(\mathbb{R}^+)}) \left| \int_0^\infty (\varphi - \psi) da \right| + \|\varphi - \psi\|_{H^{-1}(\mathbb{R}^+)} \right) \end{aligned}$$

and is uniformly bounded. Here $H^{-1}(\mathbb{R}^+)$ is the dual to $H^1(\mathbb{R}^+)$.

CONDITION 4.4. *The initial condition, $u_0(x, a)$, is bounded and nonnegative, and there exists \tilde{a}_{\max} such that $u_0(x, a) = 0$ for $a > \tilde{a}_{\max}$.*

An example of the birth condition is

$$(4.2) \quad b(x, \varphi(x, \cdot, t)) = \int_0^\infty \beta(x, a, \Phi) \varphi(x, a, t) da,$$

where $\beta \geq 0$ is the birth rate and Φ is the integral of φ with respect to age. Condition 4.3 is satisfied if β is uniformly Lipschitz continuous as a function of Φ ; if $\beta(x, a, \Phi)$, considered as a function of a , is in $H^1(\mathbb{R}^+)$, with H^1 -norm bounded independently of x and Φ ; and if $\varphi \in L^1(\mathbb{R}^+) \cap L^2(\mathbb{R}^+)$ as a function of age.

Condition 4.4 is technically convenient and seems mild in light of the exponential decay of u in age [12].

The formulation of the age- and space-discrete method is as follows. We assume that $\lim_{a \rightarrow \infty} u = 0$ [12]. Let $D = \partial_t + \partial_a$. We reuse the symbol k to denote the form

$$k(\Phi; \varphi, v) = \int_\Omega k(x, \Phi) \nabla \varphi \cdot \nabla v dx;$$

the distinction between the form and $k(x, \Phi)$ should be clear from context. In variational form, for every $v \in H^1(\Omega) \otimes (L^2(\mathbb{R}^+) \cap C(\mathbb{R}^+))$, we have

$$(4.3) \quad \int_0^\infty (Du, v) + k(p; u, v) + (\mu u, v) da = (b(x, u(x, \cdot, t)) - u(x, 0, t), v(x, 0)).$$

The form (\cdot, \cdot) denotes the L^2 inner product over Ω .

Let \mathcal{M} denote a finite dimensional subspace of $H^1(\Omega)$. Let $\{a_i\}_{i=0}^{-\infty}$ be a sequence such that $a_0 = \tilde{a}_{\max}$, $0 < a_{i+1} - a_i < \Delta a$, and $a_i \rightarrow -\infty$ as $i \rightarrow -\infty$. Let \mathcal{J} be the set of a_i 's. For a fixed nonnegative integer q , let \mathcal{C} denote the space of all piecewise continuous functions over the partition of $(-\infty, \tilde{a}_{\max}]$ defined by \mathcal{J} such that $\varphi \in \mathcal{C}$ has the property that φ restricted to (a_i, a_{i+1}) is a polynomial of degree at most q . We think of the functions in \mathcal{C} as being zero on $(\tilde{a}_{\max}, \infty)$. We define a finite dimensional space in age that moves along the characteristic curves, $da/dt = 1$:

$$(4.4) \quad \mathcal{A}(t) = \{\varphi \in L^2(\mathbb{R}^+) : \varphi(\cdot) = \psi(\cdot - t)|_{\mathbb{R}^+}, \psi \in \mathcal{C}\}.$$

This discretization will allow the numerical method to be free of numerical dispersion in age. We take $U(t) \in \mathcal{M} \otimes \mathcal{A}(t)$. For $t \notin \mathcal{J}$,

$$(4.5) \quad \int_0^\infty (DU, v) + k(P; U, v) + (\mu(x, a, P)U, v) da \\ = (b(x, U(x, \cdot, t)) - U(x, 0, t), v(x, 0))$$

for every $v(t) \in \mathcal{M} \otimes \mathcal{A}(t)$. So that U is defined across points in \mathcal{J} , we require U to be a continuous mapping of time into $L^2(\Omega) \otimes L^2(\mathbb{R}^+)$. The total population density is approximated by

$$P(x, t) = \int_0^\infty U(x, a, t) da.$$

In practice we can take the age domain to be $[0, a_{\max}]$ for some a_{\max} . This is reasonable due to the exponential decay in age of u [12].

For the computations in this paper, we used discontinuous piecewise polynomials as the approximation space in age. This corresponds to the method developed earlier in [12]. Convergence theorems in [12] and [14] give one order of superconvergence. This means that by using discontinuous piecewise polynomials and postprocessing the result to continuous piecewise linear functions we can obtain second-order convergence in age. Similarly, we can postprocess a discontinuous piecewise linear approximation to continuous piecewise cubic functions. The theorem gives third-order convergence. Results in practice show the expected fourth-order convergence [14]. An energy analysis [20, 60, 61, 65] was used to obtain the convergence results in [12] and [14].

To our knowledge, the embedding of an ADI method within step-doubling is a new technique. An analysis similar to the one conducted in [15] is needed for a rigorous convergence proof of the step-doubling ADI method and remains an area of future research. In this paper we present instead a heuristic formulation and analysis based on the “symbol” of the method; we represent the method as a rational approximation to the negative exponential and compare its closeness to the negative exponential to that of a backward Euler method.

We consider the problem

$$(4.6) \quad w' = Lw,$$

where L is a diagonalizable matrix. In the case of a nonsplit operator, if $-\lambda$ is an eigenvalue of L , we solve $w' = -\lambda w$ over a time step Δt by our method to obtain a discrete scheme of the form

$$W_n = \Sigma(\lambda\Delta t) W_{n-1},$$

where Σ is a rational function of $a\Delta t$. In our ADI method, we split L into $L_{x+0} + L_y$ per Figure 6. We denote the eigenvalues by $-\lambda_{x+0}$ and $-\lambda_y$, respectively. We generalize our symbol notation to $\Sigma(\lambda_{x+0}\Delta t, \lambda_y\Delta t)$. Equation (4.6) becomes

$$(4.7) \quad w' = L_{x+0}w + L_yw,$$

and we solve

$$(4.8) \quad w' = -\lambda_{x+0}w - \lambda_yw$$

over a time step Δt to obtain the symbol of the method.

Step-doubling applied to (4.8) has the form

$$(4.9a) \quad \frac{D_{n-1/2,x} - W_{n-1}}{\Delta t/2} = -\lambda_{x+0}W_{n-1},$$

$$(4.9b) \quad \frac{D_{n-1/2} - D_{n-1/2,x}}{\Delta t/2} = -\lambda_y D_{n-1/2,x},$$

$$(4.9c) \quad \frac{D_{n,x} - D_{n-1/2}}{\Delta t/2} = -\lambda_{x+0}D_{n-1/2},$$

$$(4.9d) \quad \frac{D_n - D_{n,x}}{\Delta t/2} = -\lambda_y D_{n,x},$$

$$(4.9e) \quad \frac{S_{n,x} - W_{n-1}}{\Delta t} = -\lambda_{x+0}W_{n-1},$$

$$(4.9f) \quad \frac{S_n - S_{n,x}}{\Delta t} = -\lambda_y S_{n,x}.$$

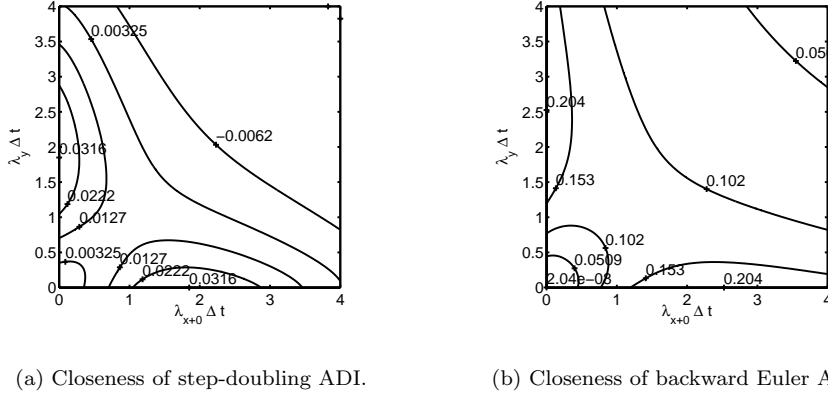


FIG. 7. Comparison of the closeness of the symbols $\Sigma_s(\lambda_{x+0}\Delta t, \lambda_y\Delta t)$ of step-doubling ADI (a) and $\Sigma_e(\lambda_{x+0}\Delta t, \lambda_y\Delta t)$ of backward Euler ADI (b) to the negative exponential $e^{-(\lambda_{x+0}\Delta t + \lambda_y\Delta t)}$. These figures show that the step-doubling ADI symbol is a second-order accurate approximation to the negative exponential and is superior in error and convergence rate to backward Euler ADI.

The computed solution at time t_n is extrapolated to $W_n = 2D_n - S_n$. This extrapolation removes the first-order error term and gives us a second-order method in time. In practice we compute each of the subsolutions to obtain D_n and S_n and then extrapolate to obtain W_n . We also compare D_n and S_n for adaptive control of the time step. Time-step control is done in the same manner as the step-doubling method without ADI. A discussion on how we conduct the time-step control is given in section 3 of [15]. The matrices L_{x+0} and L_y come from a discretization of the spatial and zero-order terms using center finite differences.

To obtain the step-doubling ADI symbol we collapse (4.9a)–(4.9f) and apply the extrapolation. The symbol is then given by

$$(4.10) \quad \Sigma_s(\lambda_{x+0}\Delta t, \lambda_y\Delta t) = 2 \left(\frac{1}{\left(1 + \frac{\lambda_{x+0}\Delta t}{2}\right) \left(1 + \frac{\lambda_y\Delta t}{2}\right)} \right)^2 - \frac{1}{(1 + \lambda_{x+0}\Delta t)(1 + \lambda_y\Delta t)}.$$

The symbol for backward Euler ADI is

$$(4.11) \quad \Sigma_e(\lambda_{x+0}\Delta t, \lambda_y\Delta t) = \frac{1}{(1 + \lambda_{x+0}\Delta t)(1 + \lambda_y\Delta t)}.$$

For a heuristic understanding of the relative performance of step-doubling ADI to an ADI method based on backward Euler, we compare the symbols Σ_s and Σ_e to the negative exponential $e^{-(\lambda_{x+0}\Delta t + \lambda_y\Delta t)}$. The results are shown in Figure 7. These results indicate the potential second-order convergence of step-doubling ADI and its superiority to backward Euler ADI.

The combined methodology of a moving-grid Galerkin method, using piecewise-continuous functions as the approximation space in age, and our step-doubling ADI method for time and space integration is second-order accurate in each of the independent variables: age, time, and space.

5. Conclusions and further research. In this paper we presented physiologically and spatially structured continuous deterministic models of cancer tumor invasion. We presented a general model whose equations depend on variables representing size, age, space, and time. We then treated a simplified model without size structure and with only two spatial dimensions. The simplified model contained one mutation class of proliferating and quiescent cells. The aim of this approach is to move tumor invasion modeling away from phenomenological models toward more mechanistic, biologically informed, and reliably predictive models. These more complex models required a more sophisticated computational methodology to investigate numerically the computationally intensive model equations.

The most immediate extension of this work is to determine the models' parameters and functional forms from biological data and experiments. The current methodology and software is sufficient to handle multiple mutation classes of proliferating and quiescent cells, but a deeper understanding of the biology is needed to benefit from this extension. Computational results from more biologically detailed models are expected, in turn, to contribute to a deeper understanding of the underlying biology.

The most important mathematical extension of the methodology is to develop size-time finite elements to handle size-structured equations. Rather than being developed for general forms of transport, extensions of the existing methods for age structure to size structure will use the specific nature of physiological change in tumor cells to allow the incorporation of size structure into a model at a low cost in terms of computational resources. Anticipated complications in handling size structure include birth in a size-structured context with respect to both the numerical methods and their analyses. Since the characteristic curves in the size-time plane are no longer lines with slope one, as was the case for age structure, some important questions are, What types of characteristic curves should we consider and how do we handle situations where these curves become asymptotically close within the moving grid framework? What happens if they meet and shocks form?

Two immediate concerns must be addressed for the problem of size dependence in tumor invasion models. The first issue is the introduction of new size nodes at the birth boundary, and the second is the handling of size intervals that contract due to the convergence of size-time characteristic curves. We expect the major complication in the size nodes to occur when growth slows as cells reach a certain size. However, because of the nonlinearities in the problem, it is insufficient to merely assume that a size interval will strictly decrease length. Addressing these two concerns will lay the foundation for methods that handle more complicated characteristics, including the formation of shocks that can form in situations where growth has complex dependencies on the physiological traits of an individual as well as the external environment.

As in the methods for age-structured systems, the moving-grid formulation is expected to account for the growth of individuals, taking the place of direct differencing of the size variable. And as in the case of age structure, the use of a space of discontinuous piecewise polynomials as the basis functions in size is expected to allow each size interval to be treated with a separate linear system. If the system has dependence on both age and size, we would have a two-dimensional array of independent linear systems at each time step.

An important benefit of using size-time Galerkin finite elements is having one mathematical framework define many methods with higher-order accuracy. Because of the need to keep computational costs down in each dimension of the high-dimension systems under study, without sacrificing robustness, the ability to choose the order of convergence of the method is quite useful.

A major extension of the software and methodology is to add a third space dimension through an additional suboperator in the ADI method. This methodology for handling three space dimensions is expected to be sufficient for generating initial results that aim to extend our understanding of tumor invasion beyond the two-dimensional space models. Other ADI methods that may work within this framework are Douglas–Gunn [59] and Strang splitting [57].

Although we have provided a specific mathematical treatment of the spatial dynamics of tumor invasion, we remark that modeling spatial dynamics can be more complicated in biological systems than in physical systems. A broad examination of different modeling approaches is required, including the continuous approach in this paper, and how it relates to other approaches, such as the HDC formulation discussed in [4]. Multiscale models of the type considered in this paper have different time scales for the dynamics at the different physical scales. For example, in the system defined in (2.1a)–(2.1f), the cellular scale gives rise to time scales in the age and size variables, whereas the tumor scale gives rise to a different time scale in the spatial variables. Independent of the specific type of spatial representation used, decoupling time from age or size is critical for effective solution of the model equations.

Many of the features of the cancer models, such as taxis, aging, and growth, are seen in other biological systems; prior work on *Proteus mirabilis* swarm-colony development is but one example [13]. Biological systems abound where either spatial dynamics induce the behavior of interest or where the spatial dynamics is the behavior of interest. In the same manner, the behavior of interest in a biological system can depend on the distribution of physiological traits such as age or size, or those distributions are the topic of interest. We hope that the methodology presented in this paper will provide a template for handling a broader range of biological problems.

REFERENCES

- [1] J. A. ADAM AND N. BELLOMO, EDS., *A Survey of Models for Tumor-Immune System Dynamics*, Modelling and Simulation in Science, Engineering, and Technology, Birkhäuser, Boston, 1997.
- [2] A. R. A. ANDERSON, *The effects of cell adhesion on solid tumour geometry*, in Morphogenesis and Pattern Formation in Biological Systems, T. Sekimura, S. Noji, N. Ueno, and P. Maini, eds., Springer-Verlag, Tokyo, 2003, pp. 315–325.
- [3] A. R. A. ANDERSON, *Solid tumour invasion: The importance of cell adhesion*, in Function and Regulation of Cellular Systems: Experiments and Models, Part VII, A. Deutsch, M. Falcke, J. Howard, and W. Zimmermann, eds., Birkhäuser, Boston, Basel, 2003, pp. 379–389.
- [4] A. R. A. ANDERSON, *A hybrid mathematical model of solid tumour invasion: The importance of cell adhesion*, Math. Med. Biol. IMA Journal, 22 (2005), pp. 163–186.
- [5] A. R. A. ANDERSON AND M. A. J. CHAPLAIN, *Continuous and discrete mathematical models of tumour-induced angiogenesis*, Bull. Math. Biol., 60 (1998), pp. 857–899.
- [6] A. R. A. ANDERSON, M. A. J. CHAPLAIN, E. L. NEWMAN, R. J. C. STEELE, AND A. M. THOMPSON, *Mathematical modelling of tumour invasion and metastasis*, J. Theoret. Med., 2 (2000), pp. 129–154.
- [7] A. R. A. ANDERSON AND A. W. PITCAIRN, *Application of the hybrid discrete-continuum technique*, in Polymer and Cell Dynamics, Part III, W. Alt, M. Chaplain, M. Griebel, and J. Lenz, eds., Birkhäuser, Boston, Basel, 2003, pp. 261–279.
- [8] O. ANGULO AND J. C. LÓPEZ-MARCOS, *Numerical schemes for size-structured population equations*, Math. Biosci., 157 (1999), pp. 169–188.
- [9] O. ANGULO AND J. C. LÓPEZ-MARCOS, *Numerical integration of fully nonlinear size-structured population models*, Appl. Numer. Math., 50 (2004), pp. 291–327.
- [10] R. P. ARAUJO AND D. L. S. MCELWAIN, *A history of the study of solid tumor growth: The contribution of mathematical modelling*, Bull. Math. Biol., 66 (2004), pp. 1039–1091.
- [11] B. P. AYATI, *BuGS 1.0 User Guide*, Tech. report CS-96-18, University of Chicago, Chicago, IL, 1996.

- [12] B. P. AYATI, *A variable time step method for an age-dependent population model with nonlinear diffusion*, SIAM J. Numer. Anal., 37 (2000), pp. 1571–1589.
- [13] B. P. AYATI, *A structured-population model of Proteus mirabilis swarm-colony development*, J. Math. Biol., 52 (2006), pp. 93–114.
- [14] B. P. AYATI AND T. F. DUPONT, *Galerkin methods in age and space for a population model with nonlinear diffusion*, SIAM J. Numer. Anal., 40 (2002), pp. 1064–1076.
- [15] B. P. AYATI AND T. F. DUPONT, *Convergence of a step-doubling Galerkin method for parabolic problems*, Math. Comp., 74 (2005), pp. 1053–1065.
- [16] N. BELLOMO AND L. PREZIOSI, *Modelling and mathematical problems related to tumor evolution and its interaction with the immune system*, Math. Comput. Modelling, 32 (2000), pp. 413–452.
- [17] A. BERTUZZI, A. D’ONOFRIO, A. FASANO, AND A. GANDOLFI, *Modelling cell populations with spatial structure: Steady state and treatment-induced evolution of tumour cords*, Discrete Contin. Dyn. Syst. Ser. B, 4 (2004), pp. 161–186.
- [18] A. BERTUZZI, A. FASANO, A. GANDOLFI, AND D. MARANGI, *Cell kinetics in tumor cords studied by a model with variable cell cycle length*, Math. Biosci., 177/178 (2002), pp. 103–125.
- [19] A. BERTUZZI AND A. GANDOLFI, *Cell kinetics in a tumor cord*, J. Theoret. Biol., 204 (2000), pp. 587–599.
- [20] S. C. BRENNER AND L. R. SCOTT, *The Mathematical Theory of Finite Element Methods*, Texts Appl. Math. 14, Springer-Verlag, New York, 1994.
- [21] S. BUSENBERG AND M. IANNELLI, *A class of nonlinear diffusion problems in age-dependent population dynamics*, Nonlinear Anal., 7 (1983), pp. 501–529.
- [22] C. CHIU, *A numerical method for nonlinear age dependent population models*, Differential Integral Equations, 3 (1990), pp. 767–782.
- [23] G. DI BLASIO, *Non-linear age-dependent population diffusion*, J. Math. Biol., 8 (1979), pp. 265–284.
- [24] G. DI BLASIO AND L. LAMBERTI, *An initial-boundary problem for age-dependent population diffusion*, SIAM J. Appl. Math., 35 (1978), pp. 593–615.
- [25] J. DOUGLAS, JR., AND T. DUPONT, *Alternating-direction Galerkin methods on rectangles*, in Numerical Solution of Partial Differential Equations - II, Academic Press, New York, London, 1971, pp. 133–213.
- [26] J. DYSON, R. VILLELLA-BRESSAN, AND G. F. WEBB, *Asynchronous exponential growth in an age structured population of proliferating and quiescent cells*, Math. Biosci., 177/178 (2002), pp. 73–83.
- [27] J. DYSON, R. VILLELLA-BRESSAN, AND G. F. WEBB, *The evolution of a tumor cord cell population*, Commun. Pure Appl. Anal., 3 (2004), pp. 331–352.
- [28] S. E. ESISOV AND J. A. SHAPIRO, *Kinetic model of Proteus mirabilis swarm colony development*, J. Math. Biol., 36 (1998), pp. 249–268.
- [29] G. FAIRWEATHER AND J. C. LÓPEZ-MARCOS, *A box method for a nonlinear equation of population dynamics*, IMA J. Numer. Anal., 11 (1991), pp. 525–538.
- [30] C. W. GEAR, *Numerical Initial Value Problems in Ordinary Differential Equations*, Prentice-Hall, Englewood Cliffs, NJ, 1971.
- [31] M. E. GURTIN, *A system of equations for age-dependent population diffusion*, J. Theoret. Biol., 40 (1973), pp. 389–392.
- [32] M. E. GURTIN AND R. C. MACCAMY, *Non-linear age-dependent population dynamics*, Arch. Rational Mech. Anal., 54 (1974), pp. 281–300.
- [33] M. E. GURTIN AND R. C. MACCAMY, *Diffusion models for age-structured populations*, Math. Biosci., 54 (1981), pp. 49–59.
- [34] M. GYLLENBERG AND G. F. WEBB, *A nonlinear structured population model of tumor growth with quiescence*, J. Math. Biol., 28 (1990), pp. 671–694.
- [35] M. A. HORN AND G. F. WEBB, EDS., *Mathematical Models in Cancer*, papers from the workshop held at Vanderbilt University, Nashville, TN, 2002; special issue in Discrete Contin. Dyn. Syst. Ser. B, 4 (2004).
- [36] C. HUANG, *An age-dependent population model with nonlinear diffusion in \mathbb{R}^n* , Quart. Appl. Math., 52 (1994), pp. 377–398.
- [37] K. ITO, F. KAPPEL, AND G. PEICHL, *A fully discretized approximation scheme for size-structured population models*, SIAM J. Numer. Anal., 28 (1991), pp. 923–954.
- [38] K. H. KARLSEN, K.-A. LIE, J. R. NATVIG, H. F. NORDHAUG, AND H. K. DAHLE, *Operator splitting methods for systems of convection-diffusion equations: Nonlinear error mechanisms and correction strategies*, J. Comput. Phys., 173 (2001), pp. 636–663.
- [39] M.-Y. KIM, *Galerkin methods for a model of population dynamics with nonlinear diffusion*, Numer. Methods Partial Differential Equations, 12 (1996), pp. 59–73.

- [40] M.-Y. KIM AND E.-J. PARK, *Mixed approximation of a population diffusion equation*, Comput. Math. Appl., 30 (1995), pp. 23–33.
- [41] K. KUBO AND M. LANGLAIS, *Periodic solutions for a population dynamics problem with age-dependence and spatial structure*, J. Math. Biol., 29 (1991), pp. 363–378.
- [42] Y. KWON AND C.-K. CHO, *Second-order accurate difference methods for a one-sex model of population dynamics*, SIAM J. Numer. Anal., 30 (1993), pp. 1385–1399.
- [43] M. LANGLAIS, *A nonlinear problem in age-dependent population diffusion*, SIAM J. Math. Anal., 16 (1985), pp. 510–529.
- [44] M. LANGLAIS, *Large time behavior in a nonlinear age-dependent population dynamics problem with spatial diffusion*, J. Math. Biol., 26 (1988), pp. 319–346.
- [45] L. LOPEZ AND D. TRIGIANTE, *A finite difference scheme for a stiff problem arising in the numerical solution of a population dynamic model with spatial diffusion*, Nonlinear Anal., 9 (1985), pp. 1–12.
- [46] J. C. LÓPEZ-MARCOS, *An upwind scheme for a nonlinear hyperbolic integro-differential equation with integral boundary condition*, Comput. Math. Appl., 22 (1991), pp. 15–28.
- [47] R. C. MACCAMY, *A population model with nonlinear diffusion*, J. Differential Equations, 39 (1981), pp. 52–72.
- [48] P. MARCATI, *Asymptotic behavior in age-dependent population dynamics with hereditary renewal law*, SIAM J. Math. Anal., 12 (1981), pp. 904–916.
- [49] A. G. MCKENDRICK, *Applications of mathematics to medical problems*, Proc. Edin. Math. Soc., 44 (1926), pp. 98–130.
- [50] R. I. MCLACHLAN AND G. R. W. QUISPEL, *Splitting methods*, Acta Numer., 11 (2002), pp. 341–434.
- [51] L. PREZIOSI, ED., *Cancer Modelling and Simulation*, Chapman & Hall/CRC, Boca Raton, FL, 2003.
- [52] O. RAUPRICH, M. MATSUSHITA, K. WEIJER, F. SIEGERT, S. E. ESİPOV, AND J. A. SHAPIRO, *Periodic phenomena in Proteus mirabilis swarm colony development*, J. Bacteriol., 178 (1996), pp. 6525–6538.
- [53] M. ROTENBERG, *Theory of population transport*, J. Theoret. Biol., 37 (1972), pp. 291–305.
- [54] L. F. SHAMPINE, *Local error estimation by doubling*, Computing, 34 (1985), pp. 179–190.
- [55] F. R. SHARPE AND A. J. LOTKA, *A problem in age-distribution*, Philos. Mag., 21 (1911), pp. 435–438.
- [56] J. G. SKELLAM, *Random dispersal in theoretical populations*, Biometrika, 38 (1951), pp. 196–218.
- [57] G. STRANG, *On the construction and comparison of difference schemes*, SIAM J. Numer. Anal., 5 (1968), pp. 506–517.
- [58] D. SULSKY, *Numerical solution of structured population models, I. Age structure*, J. Math. Biol., 31 (1993), pp. 817–839.
- [59] J. W. THOMAS, *Numerical Partial Differential Equations: Finite Difference Methods*, Texts Appl. Math. 22, Springer-Verlag, New York, 1995.
- [60] V. THOMÉE, *Galerkin Finite Element Methods for Parabolic Problems*, Springer Ser. Comput. Math. 25, Springer-Verlag, Berlin, 1997.
- [61] L. B. WAHLBIN, *Superconvergence in Galerkin Finite Element Methods*, Lecture Notes in Math. 1605, Springer-Verlag, New York, 1995.
- [62] G. F. WEBB, *An age-dependent epidemic model with spatial diffusion*, Arch. Rational Mech. Anal., 75 (1980/81), pp. 91–102.
- [63] G. F. WEBB, *Theory of Nonlinear Age-Dependent Population Dynamics*, Monogr. Textbooks Pure Appl. Math. 89, Marcel Dekker, New York, 1985.
- [64] G. F. WEBB, *α - and β -curves, sister-sister and mother-daughter correlations in cell population dynamics*, Comput. Math. Appl., 18 (1989), pp. 973–984.
- [65] M. F. WHEELER, *A priori L_2 error estimates for Galerkin approximations to parabolic partial differential equations*, SIAM J. Numer. Anal., 10 (1973), pp. 723–759.